

self-consistent force-constant change does not reduce but enhances the scattering from the mass defect. To lowest order in ω .

$$[\tau(\omega)]^{-1} = (\omega^4/4\pi)s^{-3}[\epsilon^2 - 4\gamma\epsilon(3+2\gamma)^{-1} + 12\gamma^2(3+2\gamma)^{-2}]. \quad (13)$$

For ^4He defects in ^3He , we have $\epsilon = -\frac{1}{3}$ and $\gamma \approx 0.14$. The self-consistent scattering rate is thus about twice that calculated for the mass defect only, in agreement with the experimental thermal-conductivity results reported by Callaway and by Berman and Day.⁹

As can be seen by comparing the force-constant changes with static relaxation included (Table I) and those without relaxation (Fig. 1), the relaxation effects contribute only a small part of the total force-constant change. As previously noted by Varma,² the attribution of enhanced scattering to relaxation only¹⁰ neglects the more important effect.

We are grateful for several useful conversations with Dr. C. M. Varma.

*Work partially supported by the National Science Foundation Science Development Grant No. GU 2648.

†Present address: Autonetics, 3370 Miraloma Ave., Anaheim, Calif. 92803.

¹See A. A. Maradudin, in *Solid State Physics*, edited by H. Ehrenreich, F. Seitz, and D. Turnbull (Academic, New York, 1965), Vol. 18, and *ibid.*, Vol. 19 (1966) for reviews.

²C. M. Varma, Phys. Rev. Lett. **23**, 778 (1969), and Phys. Rev. A **4**, 313 (1971).

³R. J. Elliott and D. W. Taylor, Proc. Phys. Soc., London **83**, 183 (1964).

⁴A similar approach was followed by S. Takeno, Progr. Theor. Phys., Suppl. **45**, 137 (1970).

⁵We use the two-body potential which incorporates the Jastrow function for short-range correlations, developed by L. H. Nosanow, Phys. Rev. **146**, 120 (1966).

⁶N. S. Gillis, N. R. Werthamer, and T. R. Koehler, Phys. Rev. **165**, 951 (1968).

⁷R. J. Elliott and D. W. Taylor, Proc. Roy. Soc., London **296**, 161 (1967).

⁸W. M. Hartmann, H. V. Culbert, and R. P. Huebener, Phys. Rev. B **1**, 1486 (1970).

⁹J. Callaway, Phys. Rev. **122**, 787 (1961); R. Berman and C. R. Day, Phys. Lett. **33A**, 329 (1970). By contrast, B. Bertman, H. A. Fairbank, R. A. Guyer, and C. W. White, Phys. Rev. **142**, 79 (1966), find a ratio of scattering rate to mass-defect scattering rate of 10–20. It appears to us that this discrepancy may be partly explained by the incorporation of deviations from scaling of the force constants, which leads to a term in the T matrix not proportional to ω^2 . This effect will be discussed elsewhere.

¹⁰P. G. Klemens and A. A. Maradudin, Phys. Rev. **123**, 804 (1961).

New Method of Calculating Bulk and Surface States in Thin Films*

Gerald P. Alldredge and Leonard Kleinman

Department of Physics, University of Texas, Austin, Texas 78712

(Received 17 January 1972)

We describe a new method for calculating two-dimensional energy bands in thin films. The method has the advantage that the potential varies continuously between film and vacuum regions and may even be made self-consistent. A band calculation has been performed for a 13-layer (1,0,0) Li film. We display graphs of the charge density and of the wave function of a surface state found in the $(\frac{1}{2}, \frac{1}{2}, 0)$ energy gap.

The theoretical study of the effect of crystal surfaces on crystal eigenstates dates back to the pioneering work of Tamm¹ in 1932. Most of the early work and much of the recent work has been done in the tight-binding approximation.² Because simple³ tight-binding calculations are known to be extremely poor for infinite metals and semiconductors,⁴ the method is mainly pedagogic; it shows qualitatively how surface and bulk states develop out of atomic states.⁵ Even if one could do the finite crystal with the same accuracy as

the infinite, there still remains the problem of the self-consistency of the potential; this is only beginning to be achieved in infinite-crystal tight-binding calculations.

Recently, an entirely different method has been applied by Forstmann and Heine⁶ to obtain surface states on nickel. They join smoothly the exponentially decaying wave function outside the crystal to a wave function inside the crystal made up out of all the Bloch solutions for the infinite crystal with the same energy, including those

with complex \tilde{k} 's, which decay exponentially into the crystal. This method has the shortcoming that the bulk-to-vacuum change of potential is represented by a sharp discontinuity at the crystal "surface" (located somewhat arbitrarily); in actuality, the transition region extends smoothly over perhaps three lattice constants⁷ on either side of the "surface." Another difficulty arises from the zero of energy in the bulk crystal. For infinite crystals this is a completely arbitrary quantity when the potential is calculated self-consistently. If the potential is calculated from a superposition of atomic potentials, a value of V_0 is obtained, but it is very strongly dependent on the charge distribution arising from the tails of the valence wave functions of the atom. Since these are strongly distorted when the atoms are brought together to form the crystal, this value of V_0 cannot be taken seriously. For infinite crystals, the only effect of V_0 is to shift all the bands together; and, strictly speaking, V_0 cannot even be defined for an infinite crystal since there is no reference point outside the crystal. For finite or semi-infinite crystals, V_0 is well defined and plays a major role in determining the energy of crystal states relative to the vacuum. It can be calculated self-consistently; the Forstmann-Heine method does not allow a self-consistent potential, however, and therefore must rely on the highly inaccurate atomic V_0 .

In this paper we describe a new method for calculating both surface and bulk states in thin films, which has none of the disadvantages of the methods just described. Consider a thin film, taking the origin of our coordinate system midway between the two surface planes of atoms and the coordinate x to be along the surface normal. Define a length L sufficiently large that the electronic charge density is completely negligible at a point (L, y, z) . A three-dimensional unit cell is then defined by the right parallelepiped whose base is the two-dimensional unit cell⁸ defined by a surface plane and whose altitude is $2L$. A complete set of basis functions obeying the two-dimensional periodic boundary condition and vanishing at $(\pm L, y, z)$ is then

$$\begin{aligned}\varphi_{mn}(\vec{k}) &= 2^{1/2} \exp[i(\vec{k} + \vec{G}_m) \cdot \vec{r}] \sin(\tfrac{1}{2}n\pi x/L), \\ &\quad n \text{ an even integer (odd parity),} \\ &= 2^{1/2} \exp[i(\vec{k} + \vec{G}_m) \cdot \vec{r}] \cos(\tfrac{1}{2}n\pi x/L), \\ &\quad n \text{ an odd integer (even parity),}\end{aligned}\quad (1)$$

where \vec{k} is a vector lying within the two-dimen-

sional Brillouin zone and \vec{G}_m is a two-dimensional reciprocal-lattice vector.⁹ Fairly rapid convergence of the secular determinant is obtained when the crystal potential is replaced by a weak pseudopotential, otherwise the plane-wave basis set must be replaced by orthogonalized or augmented-plane-wave basis sets. Thus the energy level calculations for thin films become almost identical to those for infinite crystals, except that the energy bands are two-dimensional and the unit cell instead of containing one or at most a few atoms contains N atoms, where N is the number of planes of atoms in the film. Any surface states present are obtained automatically along with the bulk states in the solution of the secular determinant.

We have calculated the two-dimensional energy bands of a 13-layer (1,0,0) lithium film. We took our crystal pseudopotential to be a superposition of atomic pseudopotentials of the form

$$V_{ps}(\vec{r}) = V(\vec{r})\langle\vec{r}|\psi_{1s}\rangle\langle\psi_{1s}|, \quad (2)$$

where $V(\vec{r})$ was taken from Herman and Skillman¹⁰ as was $\langle\vec{r}|\psi_{1s}\rangle$. The $\rho^{1/3}$ exchange adds a long tail to the atomic potential or a large negative peak to $V(\vec{K})$ [the Fourier transform of $V(\vec{r})$] at small \vec{K} . For infinite crystals the reciprocal-lattice vectors lie beyond this peak, and the only effect is to shift the arbitrary zero of energy. For thin films the zero of energy is not arbitrary and, furthermore, the first few wave vectors, $k_x = \frac{1}{2}n\pi/L$, lie within the peak. With the exchange peak in $V(\vec{K})$ we obtained a work function of about 3 Ry; we therefore eliminated the valence exchange contribution to Herman and Skillman's $V(\vec{r})$. We chose $A = 4.4884$ to give a $(\frac{1}{2}, \frac{1}{2}, 0)$ energy gap of 0.209 Ry in the infinite crystal, in agreement with Ham's¹¹ first-principles calculation. Although this potential is not self-consistent, it is a vast improvement over the discontinuous potentials previously used.⁶ We took a selvedge region 3 layers thick on either side of the 13-layer film; i.e., $2L = 19a/2$, where $a = 3.449 \text{ \AA}$ is the bulk lattice constant, and the (1,0,0) planes are separated by $\frac{1}{2}a$. Although our method requires only that the planes all have the same two-dimensional symmetry, we took them to be equally separated, because we have no information about relaxation of the surface planes. We took advantage of the two-dimensional symmetry by expanding in symmetrized combinations (S2DPW's) of the group of \vec{k} . We used from three to seven S2DPW's and thirty values of n , making our largest matrix 210×210 . Because of the reflection symmetry in

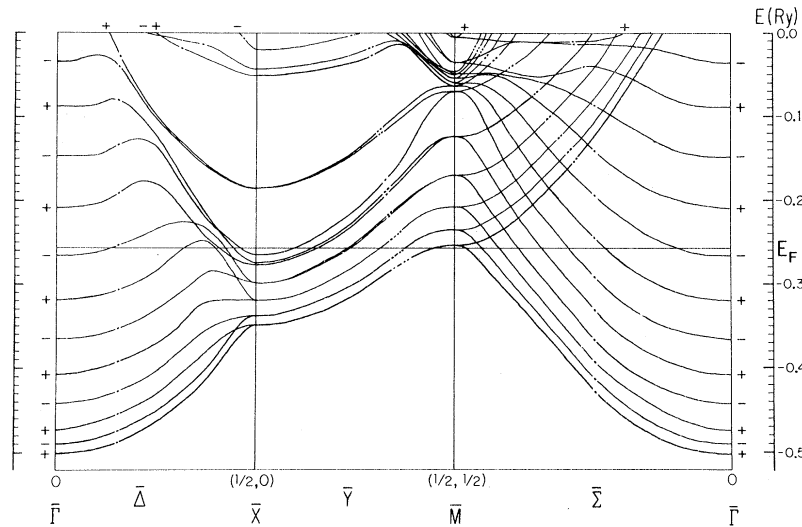


FIG. 1. Two-dimensional energy bands of 13-layer Li film. The single and double dots distinguish between \bar{Y}_1^\pm , $\bar{\Delta}_1^\pm$, $\bar{\Sigma}_1^\pm$ and \bar{Y}_2^\pm , $\bar{\Delta}_2^\pm$, $\bar{\Sigma}_2^\pm$ states, respectively. The (\pm) parity is shown at the edge of the figure. All the $\bar{\Gamma}$ states are $\bar{\Gamma}_1^\pm$. The states at \bar{X} can be determined by the compatibility relations $\bar{X}_1^\pm \rightarrow \bar{\Delta}_1^\pm$, \bar{Y}_1^\pm and $\bar{X}_3^\pm \rightarrow \bar{\Delta}_3^\pm$, \bar{Y}_2^\pm . The six lowest states at M are doubly degenerate \bar{M}_5^+ or \bar{M}_5^- , and above these are $(\bar{M}_4^+, \bar{M}_1^+)$, $(\bar{M}_4^-, \bar{M}_1^-)$, $(\bar{M}_4^+, \bar{M}_1^+)$, \bar{M}_4^- , \bar{M}_1^- , \bar{M}_4^+ , $(\bar{M}_1^+, \bar{M}_1^-)$, \bar{M}_5^+ , where states too close in energy to be distinguished in the figure are in parenthesis.

the $x=0$ plane, the n 's were all even or all odd. We studied the convergence properties of the expansion by calculating the $\bar{\Gamma}_1^+$ levels with sixty odd values of n . The resulting downward shifts varied smoothly from 0.0001 Ry for the lowest level to 0.0011 Ry for the highest negative energy level. Increasing the selva region to 6 layers (for sixty n 's) caused negligible change in all except the highest energy $\bar{\Gamma}_1^+$, which dropped another 0.0003 Ry. Finally, doubling the number of S2DPW's from 3 to 6 (for thirty n 's) caused all the levels to drop by 0.0103 to 0.0108 Ry. This rather poor planar convergence is a property of the second row of the periodic table and will not occur for heavier metals.

The two-dimensional energy bands calculated at $\bar{\Gamma}$, \bar{X} , and \bar{M} and at three points along each of the symmetry lines $\bar{\Delta}$, \bar{Y} , and $\bar{\Sigma}$ are displayed in Fig. 1. The two lowest \bar{X} levels, \bar{X}_3^+ and \bar{X}_1^+ , correspond to levels at $(0, 0, \frac{1}{2})$ in the infinite crystal. The levels above these correspond to increasing k_x in the three-dimensional case. The top level of the closely bunched group (the third \bar{X}_1^-) corresponds to $(\frac{1}{2}, 0, \frac{1}{2})$. Note that it is almost degenerate (and becomes exactly degenerate as the film becomes infinitely thick) with the lowest \bar{M}_5^+ level corresponding to $(0, \frac{1}{2}, \frac{1}{2})$ in the infinite crystal. There is then a gap of 0.215 Ry to an \bar{X}_1^+ level corresponding to the $(\frac{1}{2}, 0, \frac{1}{2})$ gap of 0.209 Ry in the infinite crystal. Within this gap

lie two¹² surface states \bar{X}_3^- and \bar{X}_3^+ .¹³ They are nearly degenerate and become exactly degenerate as the film becomes infinitely thick for the same reason that the even and odd states of the H_2 molecule become degenerate as the atoms are pulled apart. In the infinite crystal the \bar{X}_3^+ and \bar{X}_1^+ levels are degenerate. They differ by a translation from cube center to cube corner, but the cube centers and corners are indistinguishable in the infinite crystal. In the 13-layer crystal, the surface layers contain cube centers. In a 15-layer film, the surface layers contain cube corners, and \bar{X}_1 and \bar{X}_3 interchange roles¹⁴; the surface states are then \bar{X}_1^\pm . In Fig. 2 we display the $(\bar{X}_3^+)_6$

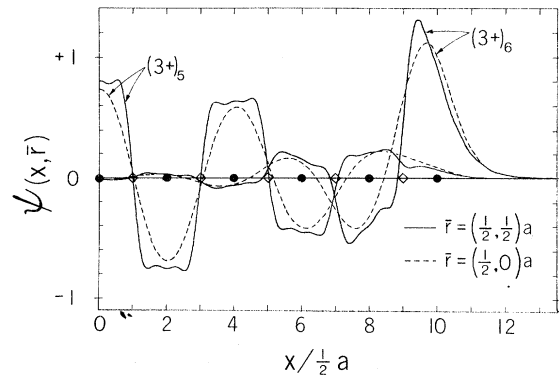


FIG. 2. The surface state $(\bar{X}_3^+)_6$ and bulk state $(\bar{X}_3^+)_5$ wave functions in a 21-layer Li film for $\bar{r} = (\frac{1}{2}, \frac{1}{2})$ and $(\frac{1}{2}, 0)$. The wave functions have nodes for $\bar{r} = (0, 0)$.

wave function of the surface state and the $(\bar{X}_3^+)_5$ state immediately below it in energy for a 21-layer film.¹⁵ The functions were obtained by summing 672 plane waves¹⁶ at various values of (x, \bar{r}) . For $(x, 0, 0)$ the \bar{X}_3 functions have a node. For $(x, \frac{1}{2}, \frac{1}{2})$ the wave functions pass through the cube corner atoms, and, responding to the rapidly varying potential, they are not at all smooth. For $(x, \frac{1}{2}, 0)$, the wave functions are as far from both the cube corner and center atoms as they can be and therefore are very smooth. Note that the $(\bar{X}_3^+)_5$ function is much smaller near the surface than an ordinary wave function, since it must be orthogonal to the $(\bar{X}_3^+)_6$ surface wave function. The $(\bar{X}_3^-)_6$ surface state is nearly identical to $(\bar{X}_3^+)_6$ near the surface, but being odd, goes to zero at $x=0$.

In Fig. 3 we display the total charge density of the 13-layer film, obtained by taking the absolute square of the wave functions¹⁶ for all the calculated states below the Fermi line¹⁸ and summing them with a weighting proportional to that fraction of the area of the two-dimensional Brillouin zone closer to \bar{k} for the particular state than to \bar{k} for any other calculated state. Note how rapidly the charge density starts to fall off even before the surface plane of atoms. This is due in part to our $V(\bar{k})$ being still too negative for small values of \bar{k} , even though we reduced it tremendously when we removed the valence exchange contribution. This is confirmed by noticing in Fig. 1 that

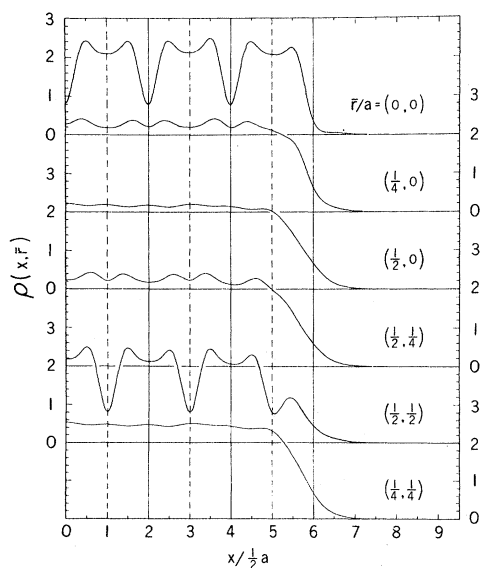


FIG. 3. Charge density (in units of electrons per a^3) for six values of \bar{r} for a 13-layer Li film. Solid and dashed vertical lines, cube center and corner planes, respectively.

$E_F = -0.257$ Ry, whereas the experimental work function is 0.183 Ry.¹⁹ This is probably not so much the fault of our atomic potential as it is of the fact that, as the charge is pulled into the crystal from the surface, it sets up a surface potential tending to oppose the further pulling in of the charge. This clearly shows the need for fully self-consistent calculations. Note also how the charge avoids the ion cores. This is because of the repulsive nature of the second term in Eq. (2) and has been observed in infinite-crystal calculations.²⁰ The $(x, 0, 0)$ and $(x, \frac{1}{2}, \frac{1}{2})$ curves which go through the cube center and corner ions, respectively, are identical deep inside the film except for a displacement of $\frac{1}{2}a$. The $(x, \frac{1}{2}, 0)$ curve, which keeps a maximum distance from all the ions, is practically flat.

It will be computationally much more difficult to achieve self-consistency in thin films than in infinite crystals. This is due in part to the larger number of plane waves in the expansion, but is mainly due to the exchange term which will undoubtedly have to be calculated in real space over the entire thin-film unit cell of dimensions $a \times a \times 2L$. Once this is done, however, it should be little more work to calculate the total energy of the film. By minimizing this total energy as a function of the relaxation of the surface layers, first-principles calculations of the surface relaxation will be obtained. Since no symmetry is required in the normal direction, the surface planes of atoms may differ from the interior atomic planes as long as they are epitaxial. Thus, a self-consistent study of the effect of surface layers on work functions is possible.

*Research supported by the U. S. Air Force Office of Scientific Research under Grants No. AF-AFOSR-68-1507 and No. AF-AFOSR-71-1973.

¹I. Tamm, Z. Phys. **76**, 849 (1932), and Phys. Z. Sowjetunion **1**, 733 (1932).

²S. G. Davidson and J. D. Levine, in *Solid State Physics*, edited by H. Ehrenreich, F. Seitz, and D. Turnbull (Academic, New York, 1970), Vol. 25, p. 1. See references therein.

³Finite-crystal work has been limited to "simple" expansions containing a minimum number of atomic functions, and has neglected all but nearest-neighbor overlap integrals.

⁴F. J. Corbato [Ph.D. thesis, Massachusetts Institute of Technology, 1956 (unpublished)] has shown that, for graphite, overlap integrals out to fifth neighbors must be included.

⁵W. Shockley, Phys. Rev. **56**, 317 (1939).

⁶F. Forstmann and V. Heine, Phys. Rev. Lett. **24**,

1419 (1970).

⁷This transition region can of course be much larger in nonmetallic crystals, where the surface charge distribution may yield a long-range potential.

⁸E. A. Wood, *Bell Syst. Tech. J.* **43**, 541 (1964).

⁹R. E. Allen, G. P. Alldredge, and F. W. de Wette, *Phys. Rev. B* **4**, 1648 (1971).

¹⁰F. Herman and S. Skillman, *Atomic Structure Calculations* (Prentice-Hall, Englewood Cliffs, N. J., 1963).

¹¹F. S. Ham, *Phys. Rev.* **128**, 82, 2524 (1962).

¹²The two surface eigenstates are even and odd combinations of surface states on each of the two surfaces of the film.

¹³These are discussed in detail in the nearly-free-electron model by L. Kleinman, to be published.

¹⁴The relationship between \bar{X}_3 and \bar{X}_1 here corresponds

to the relationship between $\beta=1$ and $\beta=-1$ in the nearly free-electron model of Ref. 13.

¹⁵We used 42 values of n for the 21-layer film. With five symmetrized combinations of planar wave vectors, we again had a 210×210 matrix to diagonalize.

¹⁶This sum of plane waves actually gives us the pseudo wave function; i.e., the very rapid oscillation of the wave function due to its orthogonality to the 1s core function is not included.

¹⁷Except for the $\bar{\Gamma}$, \bar{X} , and \bar{M} points, the wave functions are all complex.

¹⁸In two dimensions the Fermi surface becomes the Fermi line.

¹⁹P. A. Anderson, *Phys. Rev.* **75**, 1205 (1949).

²⁰W. A. Harrison, *Pseudopotentials in the Theory of Metals* (Benjamin, New York, 1966). See Fig. 6-7.

Optical Detection of Paramagnetic Resonance in the Excited State of F Centers in CaO^\dagger

P. Edel, C. Hennies,* Y. Merle D'Aubigné, R. Romestain, and Y. Twarowski‡

Laboratoire de Spectrométrie Physique, 38 Grenoble-Gare, France

(Received 7 March 1972)

A detailed analysis of this double-resonance experiment shows that the emission takes place from the 3P excited level whose degeneracy is lifted by the Jahn-Teller coupling to E_g modes of vibration. An energy-level crossing effect is observed and its origin discussed.

From the structural point of view the F center in the alkali halides is one of the simplest point defects. As such it has served as a model for many theories and as a test for new experimental techniques. The F' center (two electrons in an anion vacancy), though nearly as simple, has received much less attention since its ground-state level is nonmagnetic and its first excited level is not bound. One of the interesting results in the recent development of the study of the point defects in the alkaline-earth oxides is that, because of the extra charge of the vacancy, the two electrons of the F center¹ are more tightly bound and the first excited level is a bound state. The energy-level scheme of these centers is analogous to the one for the helium atom. In CaO the $^1S \rightarrow ^1P$ transitions give rise to a strong absorption band at 4000 \AA . On the basis of calculations by Neeley and Bartram, Henderson, Stokowski, and Ensign² have attributed the fluorescence band observed around 6000 \AA to the $^3P \rightarrow ^1S$ transitions. Using an optical detection technique³ we observed the paramagnetic resonance in this metastable level. Three equivalent tetragonal spectra were observed, showing that the orbital degeneracy is lifted either by Jahn-Teller coupling to E_g modes of vibration or by static deformations. The spec-

trum confirms that the emitting level is a spin triplet. Good agreement is found between the values of the spin-orbit coupling constant deduced from the lifetime and from the measured parameters of the spin Hamiltonian. We observed many effects similar to those taking place in excited triplet states of molecular crystals. For instance, the variation with magnetic field of the polarization of the fluorescence light clearly shows the effect of the crossing of Zeeman sublevels.

The measurements were carried out using apparatus described elsewhere.⁴ Slight modifications allowed detection of the fluorescence light in directions perpendicular or parallel to the magnetic field which is produced by a 12-in. Varian magnet. The microwave cavity is immersed in the He bath of a metallic cryostat. It is rectangular or cylindrical for frequencies in the X or K bands, respectively. The analysis of the circular polarization of the emitted light is made through a piezo-optical modulator analogous to the one described by Jaspersen and Schnatterly.⁵ It can be transformed into a linear polarization analyzer by adding a quarter-wave plate. The photomultiplier signal is then detected in phase with the modulation. Two techniques may be used to detect the resonance in the excited level: (a)